Inorg. Chem. **2005**, *44*, 7171–7174

Coordinatively Induced Length Control and Photoluminescence of $W_{18}O_{49}$ Nanorods

Kyoungja Woo,*,† Jangwon Hong,† Jae-Pyoung Ahn,† Jong-Ku Park,† and Kang-Jin Kim‡

Nano-Materials Research Center, Korea Institute of Science and Technology, P.O. Box 131, Cheongryang, Seoul 130-650, Korea, and the Department of Chemistry, Korea University, 5-1 Anam-Dong, Sungbook-Ku, Seoul 136-701, Korea

Received March 29, 2005

A coordinatively induced length control of $W_{18}O_{49}$ nanorods has been developed using thermal decomposition of $W(CO)_6$ in octyl ether solutions of single or mixed capping agents, oleic acid (OA), oleic acid/hexadecylamine (HDA), and oleic acid/trioctylphosphine oxide (TOPO). The order of length for nanorods synthesized with different capping agents was OA > OA/HDA > OA/TOPO, which was the opposite of order of their coordinating power. The order of crystalline size (diameter × length) from the TEM image was OA/HDA > OA > OA/TOPO and matched exactly with the order of crystallinity from the XRD pattern. The order of photoluminescence intensity was OA/HDA < OA < OA/TOPO and was the opposite of the order for the crystalline size or crystallinity. The strong coordinating power and steric bulkiness of TOPO is thought to interrupt the growth of the nanorods, the rearrangement of the end face atoms, and the fusion of the lateral faces and, thereby, increase the oxygen defects and the photoluminescence intensity.

Introduction

Oxygen-deficient nonstoichiometric tungsten oxides (WO_{3-x}) have attracted much attention because their optochromic, electrochromic, and gaschromic properties are utilized in the fields of catalysts,[1] electrochemistry,[2] gas sensors,[3] etc. Also, they have been used as precursors for tungsten carbides[4] and WS_2 nanotubes.[5]

Among the various WO_{3-x}, monoclinic $W_{18}O_{49}$ is one of the most investigated because of its unusual defect structure and promising properties in the nanometer regime.[6,7] The monoclinic $W_{18}O_{49}$ consists of an ordered 2-D lattice of edge-sharing WO_6 octahedra forming a network of pentagonal columns interspersed with hexagonal channels.[8,9] This phase is not only highly anisotropic but also possesses the mechanical strength necessary to hold the brittle oxide nanowhiskers together during their growth.[8] Actually, the $W_{18}O_{49}$ nanoparticles have been reported to be rods or whiskers in most of the literature.[6−11] In a recent solution-based synthesis,[6] the longer $W_{18}O_{49}$ nanorods were synthesized at higher temperatures and exhibited the higher luminescence intensity. They suggested that the longer nanorods have more oxygen defects and therefore show higher luminescence intensity.

In this paper, we demonstrate a capping agent-driven length-controlled synthesis of $W_{18}O_{49}$ nanorods using the

* To whom correspondence should be addressed. E-mail: kjwoo@kist.re.kr.
† Nano-Materials Research Center, Korea Institute of Science and Technology.
‡ Department of Chemistry, Korea University.

(1) (a) Sayama, K.; Mukasa, K.; Abe, R.; Abe, Y.; Arakawa, H. *Chem. Commun*. **2001**, 2416. (b) Sohn, J. R.; Cho, H. S.; Kim, H. W. *J. Ind. Eng. Chem*. **1999**, *5*, 1.
(2) Bock, C.; MacDougall, B. *Electrochim. Acta* **2002**, *47*, 3361.
(3) (a) Moulzolf, S. C.; Legore, L. J.; Lad, R. J. *Thin Solid Films* **2001**, *400*, 56. (b) Berger, O.; Hoffmann, T.; Fischer, W.-J.; Melev, V. *J. Mater. Sci.: Mater. Elect*. **2004**, *15*, 483. (c) Qu, W. M.; Wlodarski, W. *Sens. Actuators, B* **2000**, *64*, 42.
(4) Swift, G. A.; Koc, R. *J. Mater. Sci*. **2000**, *35*, 2109.
(5) Rothschild, A.; Frey, G. L.; Homyonfer, M.; Tenne, R.; Rappaport, M. *Mater. Res. Innovat*. **1999**, *3*, 145.
(6) Lee, K.; Seo, W. S.; Park, J. T. *J. Am. Chem. Soc*. **2003**, *125*, 3408.
(7) (a) Zhu, Y. Q.; Hu, W.; Hsu, W. K.; Terrones, M.; Grobert, N.; Hare, J. P.; Kroto, H. W.; Walton, D. R. M.; Terrones, H. *Chem. Phys. Lett*. **1999**, *309*, 327. (b) Hudson, M. J.; Peckett, J. W.; Harris, P. J. F. *J. Mater. Chem*. **2003**, *13*, 445. (c) Li, X. L.; Liu, J. F.; Li, Y. D. *Inorg. Chem*. **2003**, *42*, 921. (d) Gu, G.; Zheng, B.; Han, W. Q.; Roth, S.; Liu, J. *Nano Lett*. **2002**, *2*, 849. (e) Hu, W. B.; Zhu, Y. Q.; Hsu, W. K.; Chang, B. H.; Terrones, M.; Grobert, N.; Terrones, H.; Hare, J. P.; Kroto, H. W.; Walton, D. R. M. *Appl. Phys. A* **2000**, *70*, 231. (f) York, A. P. E.; Sloan, J.; Green, M. L. H. *Chem. Commun*. **1999**, 269. (g) Zhang, H.; Feng, M.; Liu, F.; Liu, L.; Chen, H.; Gao, H.; Li, J. *Chem. Phys. Lett*. **2004**, *389*, 337.
(8) Frey, G. L.; Rothschild, A.; Sloan, J.; Rosentsveig, R.; Popovitz-Biro, R.; Tenne, R. *J. Solid State Chem*. **2001**, *162*, 300.
(9) Berger, O.; Fischer, W.-J.; Melev, V. *J. Mater. Sci.: Mater. Elect*. **2004**, *15*, 463.
(10) Lou, X. W.; Zeng, H. C. *Inorg. Chem*. **2003**, *42*, 6169.
(11) Li, Y.; Bando, Y.; Golberg, D. *Adv. Mater*. **2003**, *15*, 1294.

10.1021/ic0504644 CCC: $30.25
Published on Web 08/31/2005

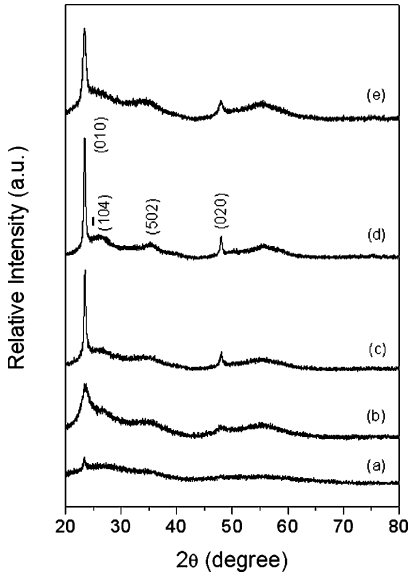

Figure 1. XRD patterns of tungsten oxide nanoparticles with various capping agents: (a) HDA, (b) TOPO, (c) OA, (d) OA/HDA, and (e) OA/TOPO.

thermal decomposition of $W(CO)_6$ in a series of hot capping agent solutions and the resultant optical properties.

Experimental Section

For a typical synthesis of $W_{18}O_{49}$ nanoparticles, 10 mL of octyl ether (Aldrich, 99%) was added to a mixture of $W(CO)_6$ [0.528 g (1.50 mmol), Acros, 99%] and oleic acid [1.43 mL (4.51 mmol), Aldrich, 90%], and this suspension was heated to 100 °C to yield a colorless solution. To this, 0.451 g (6.00 mmol) of trimethylamine *N*-oxide (Aldrich, 98%) was added and the solution was refluxed for 24 h. While the mixture was heated, the solution turned yellow, green, and then dark blue. After the solution was cooled, the nanoparticles were washed and separated with excess ethanol and centrifugation, and then, they were dried in the air. For a series of length-controlled syntheses, oleic acid was substituted by the same moles of another capping agent [HDA (Aldrich, 90%) or TOPO (Aldrich, 99%)] or a mixed capping agent (1:1 molar ratio of OA/HDA or OA/TOPO).

The X-ray diffraction (XRD) patterns were taken on Rigaku RINT/DMAX-2500 using Cu Kα radiation. Transmission electron microscopy/high-resolution transmission electron microscopy (TEM/HRTEM) images were acquired from Philips CM 200. For TEM/HRTEM analysis, 10 mg of nanoparticles was dispersed in 10 mL of hexanes. A drop of this solution was put onto a carbon-coated copper grid at room temperature and dried naturally. The FT-IR spectra were recorded using a Mattson IR 300 spectrometer with a KBr pellet. The thermal gravimetric analysis (TGA) was performed with Netzsch TG 209 F1. The heating rate was 10 °C/min under argon gas flow. The photoluminescence spectra were obtained using a ISS K2 fluorometer with excitation at 275 nm from a solution made from 0.04 g nanorod/L CH_2Cl_2.

Results and Discussion

Figure 1 shows the XRD patterns of tungsten oxide nanoparticles. The particles prepared with OA as a capping agent were highly crystalline, whereas those prepared with HDA or TOPO were amorphous to very weakly crystalline. However, the particles synthesized with 1:1 mixture of OA/HDA or OA/TOPO were highly crystalline. With no capping agent, the particles were totally amorphous. Therefore, the capping agent OA seems to be a requirement for the crystallization of tungsten oxide nanoparticles in this particular system. Also, the XRD patterns suggest that the order of crystallinity for the nanorods with the various capping agents is OA/HDA > OA > OA/TOPO. All of the crystalline nanoparticles were monoclinic $W_{18}O_{49}$, and the diffraction intensity from (010) plane was dramatically higher than that from the bulk sample.[12] This XRD pattern implicates that the crystalline $W_{18}O_{49}$ nanoparticles are rod-shaped or whiskers with a growth direction of ⟨010⟩.

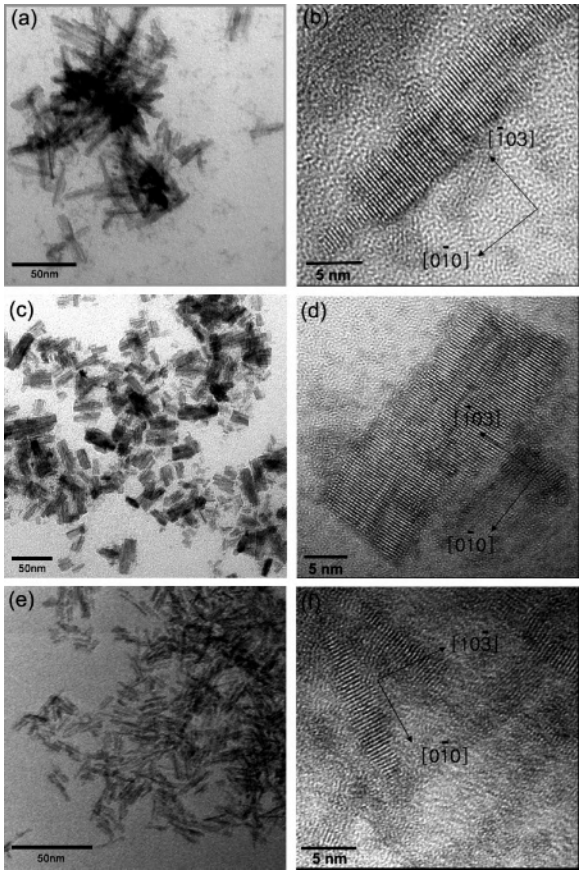

Figure 2. TEM and HRTEM images of $W_{18}O_{49}$ nanoparticles with various capping agents: (a) and (b) OA, (c) and (d) OA/HDA, and (e) and (f) OA/TOPO.

Figure 2 shows the TEM and HRTEM images of the $W_{18}O_{49}$ nanoparticles. The TEM image of nanoparticles with HDA was vague with a major part of quasi-spheres and a minor part of nanorods (Supporting Information). The image of nanoparticles with TOPO showed rudimentary quasi-spheres (Supporting Information). The sizes of the nanorods in panels a, c, and e of Figure 2, synthesized with OA, OA/HDA, and OA/TOPO, were $6.9 \pm 0.9 \times 52.2 \pm 10.9$, $16.3 \pm 3.7 \times 36.4 \pm 8.7$, and $3.8 \pm 1.0 \times 18.0 \pm 4.2$ nm, respectively. The order of length for the nanorods shown in the figure was a > c > e and was the opposite of the order of the ligand (capping agent) coordinating power,[13] which is generally known as OA < HDA < TOPO. It is suggested

(12) Powder diffraction File 05-0392 for monoclinic $W_{18}O_{49}$ (1995 JCPDS-International Center for Diffraction Data).

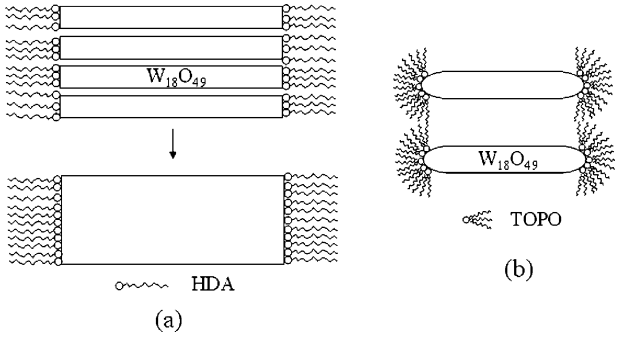

Figure 3. Suggested model for the interaction of the nanorod end face with different capping agents (HDA and TOPO). OA, which is capping the lateral face, is omitted for clarity.

that the end faces of the nanorods differentiate the three ligands and show higher selectivity for a strongly coordinating ligand. The strongly coordinating ligand protects the end face from growing more effectively than the weakly coordinating ligand. Therefore, the length of the nanorods with various coordinating ligands is considered to be the opposite of the order of the ligand coordinating power. The right column of Figure 2 shows the HRTEM image corresponding to each TEM image on the same row. As we expected from the dramatically higher (010) intensity in the XRD patterns, the direction of the growth of the nanorods was ⟨010⟩ and the lattice spacing along ⟨010⟩ was 0.378 nm in all cases.

Interestingly, TEM image c, with OA/HDA, shows a rectangle-plate shape. On the other hand, TEM images a and e show no rectangle shape. It seems that the lateral faces of the nanorods with OA/HDA are parallel aligned and fused into a single rectangle plate once the individual nanorod has grown (Supporting Information Figure S2). The HDA ligand is likely to coordinate to the (010) plane with coordinating power appropriate for similarly controlling the length, and the linear structure of the HDA ligand facilitates its self-assembly on the end face of both the individual nanorod and the resultant rectangle plate, as suggested in Figure 3a. However, the nanorods with only OA were scattered randomly because the interaction between the end face and the OA ligand was very weak. Still, their lateral faces can be fused partially as shown in HRTEM image b. It has been known that the lateral fusion of $W_{18}O_{49}$ nanorods leads to a parallel-aligned platelike nanoneedles or microbundles during the CVD process[14] and to a nanosheet in the solvothermal synthesis with no capping agent.[15] The monoclinic $W_{18}O_{49}$ networking property of pentagonal columns interspersed with hexagonal channels[8,9] is not only highly anisotropic but also possesses a mechanical strength necessary for holding the brittle oxide nanowhiskers together during their growth.[8] In our system, the lateral faces seem to fuse together because the networking property of the monoclinic $W_{18}O_{49}$ is strong and overcomes the weak interaction between the lateral face

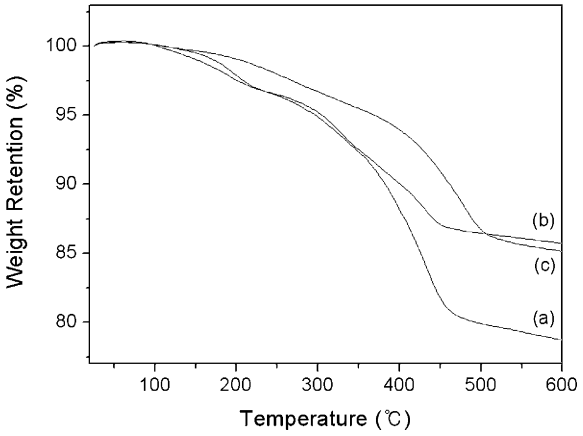

Figure 4. TGA results for $W_{18}O_{49}$ nanorods with various capping agents: (a) OA, (b) OA/HDA, and (c) OA/TOPO.

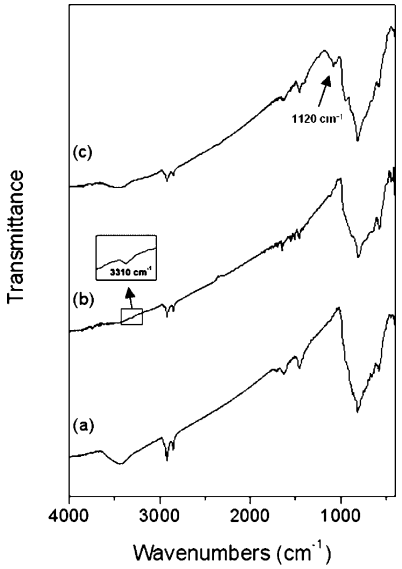

Figure 5. FT-IR spectra of $W_{18}O_{49}$ nanorods with various capping agents: (a) OA, (b) OA/HDA, and (c) OA/TOPO.

and OA. In case of the nanorods with OA/TOPO, the coordinating power of TOPO on the (010) plane is strong enough to keep the length short. However, the bulky structure of TOPO is likely to prohibit the lateral faces from making a close contact each other as suggested in Figure 3b.

Figure 4 shows the TGA results of $W_{18}O_{49}$ nanorods with various capping agents. The weight decreases around 195 °C and 330 °C corresponds to the evaporation of OA (boiling point 195 °C) and HDA (boiling point 330 °C), respectively. There seems to be a continuous decomposition of the capping ligand around 200−480 °C. The OA-capped nanorod shows a much larger weight decrease (about 20%) than that of the other nanorods (about 13%). This, together with the XRD analysis suggesting that OA is required for the nanorod crystallization, implicates that the lateral faces are capped with OA in all nanorods. When the lateral faces are in contact, they seem to fuse and grow to a single crystallite as shown in the HRTEM images (Figure 2b and d and Supporting Information).

Figure 5 shows the FT-IR spectra of $W_{18}O_{49}$ nanorods with various capping agents. All spectra display a strong broad

(13) Douglas, B.; McDaniel, D. H.; Alexander, J. J. *Concepts and Models of Inorganic Chemistry*, 2nd ed.; John Wiley & Sons: Mississauga, Canada, 1983.
(14) Jin, Y. Z.; Zhu, Y. Q.; Whitby, R. L. D.; Yao, N.; Ma, R.; Watts, P. C. P.; Kroto, H. W.; Walton, D. R. M. *J. Phys. Chem. B* **2004**, *108*, 15572.
(15) Choi, H. G.; Jung, Y. H.; Kim, D. K. *J. Am. Cer. Soc.* **2005**, *88*, 1684.

W−O band[16] around 800 cm^{-1} and metal carboxylate bands[16] around 1450 and 1550 cm^{-1}. This is considered to be a manifestation of OA coordination to $W_{18}O_{49}$ nanorods. The relative intensity of the metal−carboxylate bands has been decreased in b and c compared to that in a because of the decreased amount amount of OA. Instead, the spectra (b and c) with respective OA/HDA and OA/TOPO capping agents show the coordinated N−H band at 3310 cm^{-1} and the coordinated P═O band[17] at 1120 cm^{-1}.

Figure 6 shows the photoluminescence spectra of the $W_{18}O_{49}$ nanorods with various capping agents. The broad emission band at 370−500 nm seems to correspond to the photoluminescence from oxygen defects.[6] The order of the intensity of the photoluminescence for the nanorods with various capping agents was OA/HDA < OA < OA/TOPO and was opposite of the order of the crystalline size or crystallinity. It has been well-known that the size and shape of nanomaterials affect the physicochemical properties. The nanorods with OA/TOPO give the smallest crystal diameter and length and, therefore, possess the highest population of oxygen defects. On the other hand, the size of the crystal with OA/HDA is much larger, and the fewest oxygen defects can be expected.

In summary, a novel route for coordinatively induced length control of $W_{18}O_{49}$ nanorods has been successfully developed using the thermal decomposition of $W(CO)_6$ in a series of capping-agent solutions. The photoluminescence intensity of the smallest $W_{18}O_{49}$ nanorods with OA/TOPO was the highest. The strong coordinating power and steric hindrance of TOPO was attributed to the smallest crystalline size and the highest population of oxygen defects and, thereby, the highest photoluminescence intensity.

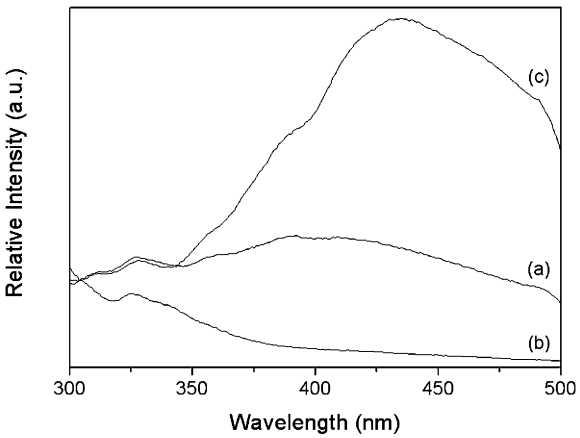

Figure 6. Photoluminescence spectra of $W_{18}O_{49}$ nanorods with various sizes and capping agents: (a) medium size and OA, (b) the largest size and OA/HDA, and (c) the smallest size and OA/TOPO.

Acknowledgment. We thank the financial support from the Korean Ministry of Science and Technology through the "National R&D Project for Nano Science and Technology".

Supporting Information Available: TEM images of $W_{18}O_{49}$ nanoparticles with various capping agents. This material is available free of charge via the Internet at http://pubs.acs.org.

IC0504644

(16) Nyquist, R. A.; Kagel, R. O. *Infrared Spectra of Inorganic Compounds*; Academic Press: San Diego, 1977.
(17) (a) Moloto, M. J.; Revaprasadu, N.; O'Brien, P.; Malik, M. A. *J. Mater. Sci.: Mater. Elect.* **2004**, *15*, 313. (b) Smythe, L. E.; Whateley, T. L.; Werner, R. L. *J. Inorg. Nucl. Chem.* **1968**, *30*, 1553.